Supporting Information

Modeling Mechanochemical Reaction Mechanisms

Heather Adams[1], Brendan P. Miller[2], Octavio J. Furlong[3], Marzia Fantauzzi,[4,5] Gabriele Navarra[4,5], Antonella Rossi,[4,5] Yufu Xu,[6] Peter V. Kotvis[1] and Wilfred T. Tysoe[1 *]

[1] Department of Chemistry and Laboratory for Surface Studies, University of Wisconsin-Milwaukee, Milwaukee, WI 53211, USA.

[2] Chevron Oronite Company LLC, 100 Chevron Way, Richmond, CA 94802, USA.

[3] INFAP/CONICET, Universidad. Nacional de San Luis, Ejército de los Andes 950, 5700 San Luis, Argentina.

[4] Dipartimento di Scienze Chimiche e Geologiche, Università degli Studi di Cagliari, Campus di Monserrato S.S. 554, Italy.

[5] INSTM, UdR, Cagliari, 09100 Italy.

[6] Institute of Tribology, School Mechanical and Automotive Engineering, Hefei University of Technology, Hefei 230009, China.

* E-mail: wtt@uwm.edu

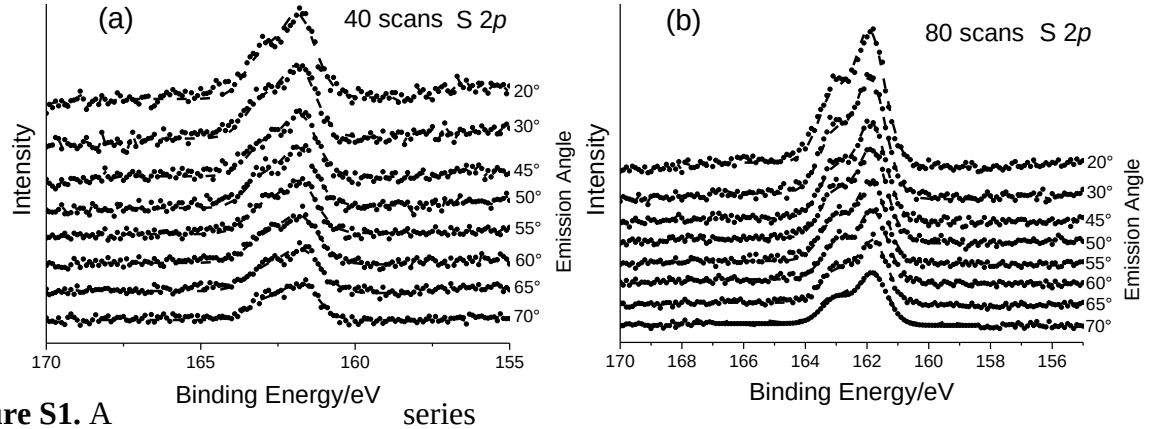

Figure S1. A series of small-spot size S 2*p* angle-resolved XPS spectra inside the rubbed region taken using a pass energy of 112 eV after rubbing the copper sample after the completion of a run-in period in the presence of a background pressure of 5×10^{-8} Torr of dimethyl disulfide for (a) 40 and (b) 80 scans at a load of 0.44 N and a sliding speed of 4 mm/s at a sample temperature of 290 K. The spectra were collected at various emission angles, referenced to the surface normal, where the angles are displayed adjacent to the corresponding spectrum.

S.1 Experimental Protocols

Measurement of Total Subsurface Sulfur: The total amount of sulfur in the subsurface region was measured using a previously developed strategy,[1] which takes advantage of the fact that sulfur is more stable on the surface than in the subsurface region so that heating the sulfur-containing sample *in vacuo* will cause any subsurface sulfur to diffuse to the surface. This experiment was carried out after rubbing the sample a number of times in the presence of 5×10^{-8} Torr of DMDS at a load of 0.44 N and a sliding speed of 4mm/s at a sample temperature of 290 K. Initially, any surface sulfur is carefully removed by Argon ion bombardment until no sulfur was detected on the unworn region of the sample by Auger spectroscopy (~120 s with a beam energy of 3 keV, 1 $\mu A/cm^2$). The sample was then heated to ~750 K and then allowed to cool to ~300 K, a process which took approximately 300 s. This caused sulfur to diffuse to the surface and spread outside the unrubbed region. The S(KLL)/Cu(LMM) Auger ratio was measured at various points across this region and integrated to yield the total amount of subsurface sulfur.

This was calibrated with respect to the integrated area of the decrease in sulfur signal profile for a monolayer of methyl thiolate species on the surface, obtained by saturating it with DMDS, after having rubbed the sample 70 times at a load of 0.44 N at a speed of 4 mm/s. This has previously been shown to transport all the sulfur from the methyl thiolate species into the bulk of the sample.[1]

XPS Measurements. The sample was transferred into the XPS vacuum chamber via a nitrogen-filled glove bag. The sample was mounted in a glove box using a PHI sample holder and attached to a transfer vessel that was stored in an external vacuum line until a pressure of ~8×10^{-10} Torr was achieved. The sample was then transferred to the spectrometer minimizing the exposure to air. Spectra were acquired with a Quantera^{SXM} (ULVAC-PHI, Chanhassen, MN, USA). This spectrometer allows small-area XP spectra to be collected in angle-resolved XPS mode with a spatial resolution ≤ 9 μm. In this work, the beam size was ~50 μm in diameter (Al Kα 1486.6 eV, X-ray power, 10.3W) and is much smaller than the rubbed region. Angle-resolved XPS (ARXPS) spectra were collected at various emission angles, measured with respect to the surface normal, from 20° to 70°. The PHI Quantera^{SXM} provides eucentric tilt at the analysis point, which simplifies the automation of angle-resolved experiments by maintaining the analysis area at the focal point of the X-ray source and analyzer for all emission angles. The calibration of the eucentric was performed immediately before spectral acquisition. The spectra were acquired in constant-analyzer-transmission mode, the pass-energy being set to 112 eV and the step size to 0.1 eV. The full-width at half-maximum (FWHM) of the peak height for Ag $3d_{5/2}$ signal was 0.9 eV under this condition. The XPS spectra were fitted using Gaussian–Lorentzian profiles after non-linear background subtraction[2-3] using CASA XPS software (CASAsoftware Ltd., UK). The asymmetry due to spin–orbit splitting was also taken into account when

processing the S 2*p* spectra. The areas of the photoelectron peaks (intensities) were corrected for photoionization cross-section,[4] angular asymmetry function,[5] and Quantera^{SXM} intensity/energy response function (IERF) for the quantitative analysis; the corrected intensities were normalized to unity for each angle and plotted versus the emission angle: this diagram is called *apparent concentration diagram*.

Depth Profiles and the Maximum Entropy Method. The aim of the maximum entropy method is to reconstruct a concentration *versus* depth profile that reflects the experimental ARXPS data, but contains the minimum amount of information required for it. The reconstruction of a depth profile from ARXPS data is an ill-posed mathematical problem, but the entropy can be used as a regularizing function (which must be maximized) to constrain the solution in order to obtain the simplest possible depth profile that matches the experimental data. A more detailed description is provided elsewhere.[6] As input to the MEM algorithm, the intensities, corrected for the photoionization cross-sections, the asymmetry function, and the transmission function were used. The electron inelastic mean free paths were calculated for each element following Seah and Dench semi-empirical approach.[7] The resulting depth profile is shown in Figure S2.

This reveals that sulfur has penetrated the subsurface region of the copper to form Cu(I) species. However, in order to compare more directly with the mechanochemical model, the variation in integrated intensities of the S 2p features was plotted against emission angle and directly compared with the predictions of the kinetic model described in Section S3 (Figure 7). To take account of differences in the absolute detection intensities for spectra measured on different portions of the surface, the signal intensities collected after 40 scans were scaled by a factor of 1.31 and those collected after 80 scans by a factor of 0.84 relative to the intensities measured after 160 scans.

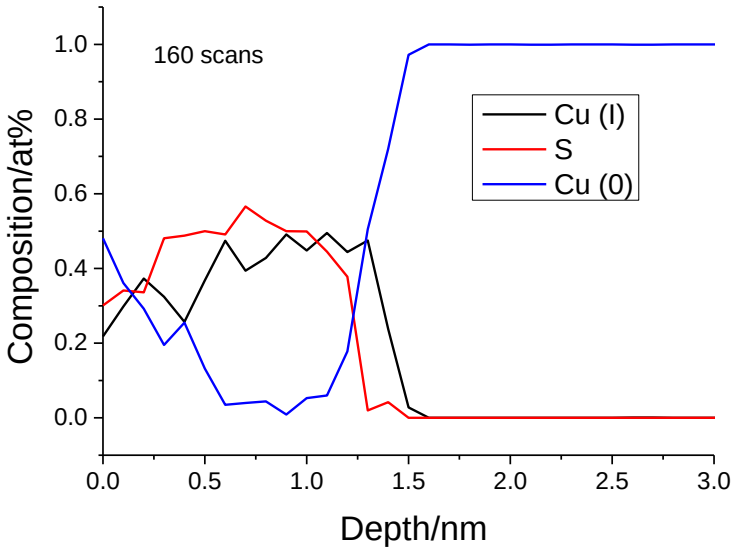

Figure S2: Calculated depth distribution of sulfur, Cu(I) and Cu(0) from the angle-resolved XPS data collected after rubbing a clean copper sample after the completion of a run-in period in the presence of a background pressure of 5×10^{-8} Torr of dimethyl disulfide for 160 scans at a load of 0.44 N and a sliding speed of 4 mm/s and T = 290 K.

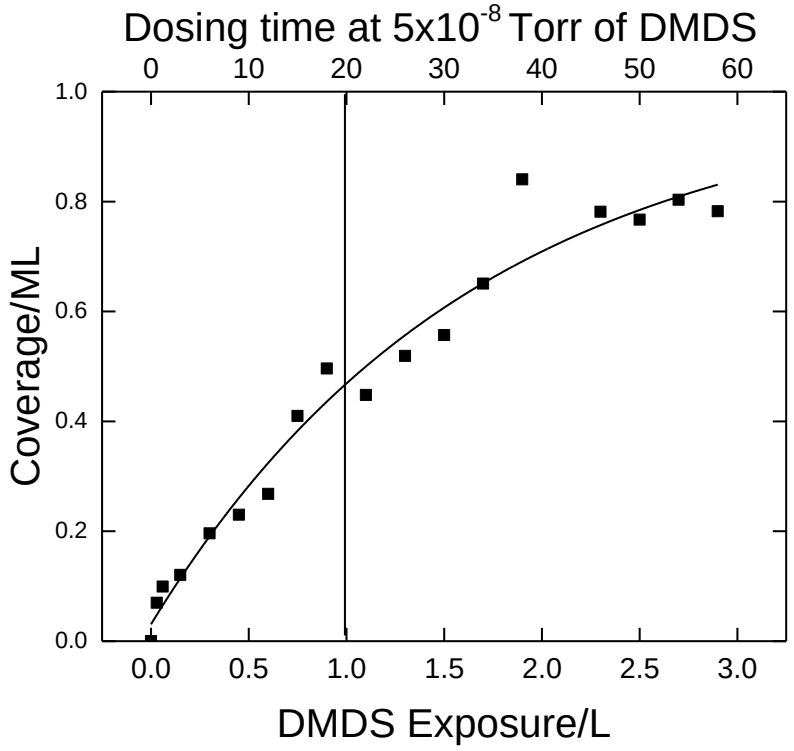

Figure S3: Plot of the methyl thiolate coverage inside a previously rubbed region of the sample as a function of dimethyl disulfide exposure in Langmuirs (1 L (Langmuir) = 1×10^{-6} Torr·s) at a sample temperature of 290 K, where the pressures are not corrected for ionization gauge sensitivity. The methyl thiolate coverage is measured from the S KLL Auger peak-to-peak intensity and the data are fit to Langmuir adsorption kinetics to obtain the relative methyl thiolate coverage. The top axis plots the dosing time at a background pressure of 5×10^{-8} Torr required to obtain the exposures shown on the bottom axis.

S2. Modeling Mechanochemical Reaction Kinetics

The sample is dosed after the completion of the run-in period in which the clean surface is rubbed at a normal load of 0.44 N at a sliding speed of 4×10^{-3} m/s at a sample temperature of ~290 K, leading to the formation of a wear track. This results in a decrease in friction coefficient of the clean surface from ~0.8 to a value of ~0.5 after ~70 passes over the surface, which remains constant at this value thereafter. This is accompanied by the formation of a wear track which grows in width during this initial run-in period to reach a constant value of ~100 μm. Assuming

that the contact deforms elastically leads to a contact pressure of ~100 MPa, while assuming plastic deformation at the contact asperities leads to a contact pressure of ~450 MPa.[8]

After completion of the run-in period, the sample was exposed to a background pressure of 5×10^{-8} Torr of DMDS while rubbing was continued and the friction coefficient monitored during each scan. DMDS reacts on the surface to form methyl thiolate species. The initial methyl thiolate coverage during the first scan is given by Θ_{th}^{0} and the initial sulfur coverage is zero. The value of Θ_{th}^{0} depends on the DMDS pressure and the interval between the time that the gas is introduced and the first pass of the pin over the surface, and is taken to be an adjustable parameter. To explore the adsorption kinetics of methyl thiolate species on the rubbed region, a wear track was formed on a clean copper sample, which was then exposed to gas-phase DMDS at a sample temperature of 290 K and the relative coverage of the resulting methyl thiolate species measured using Auger spectroscopy within the wear track from the S(KLL)/Cu(LMM) Auger intensities. The results are plotted in Figure S3 as a function of the exposure (DMDS Pressure (in Torr) × Exposure time (in seconds)), displayed in units of Langmuir (L, $1L = 1\times10^{-6}$ Torr·s). The data were fit to Langmuir adsorption kinetics in which the sticking probability at some coverage Θ, $S(\Theta)$ is given by $S(\Theta) = S_0(1-\Theta)$, where S_0 is the initial sticking probability of methyl thiolate species on a clean surface. If the gas-phase pressure is G, then the DMDS collision frequency on the surface is proportional to G, so that for adsorption onto the clean surface:

$$\frac{d\Theta_{th}}{dt} = K(1-\Theta_{th})G \qquad \text{(S1)},$$

where Θ_{th} is the methyl thiolate coverage and $K$is a constant. For a DMDS exposure time, t_{exp}, the total exposure $E = Gt_{exp}$ and:

$$\int_0^{\Theta_{th}^0} \frac{d\Theta_{th}}{1-\Theta_{th}} = KG\int_0^{t_{exp}} dt \qquad \text{(S2)},$$

and integration yields $\Theta_{th}^{0} = 1 - \exp(-KE)$. This function is fit to the data in Fig. S3, and the good fit indicates that methyl thiolate adsorbate *via* Langmuir kinetics. Based on the data shown in Fig. S3, Θ_{th}^{0} is expected to lie between ~0.2 and 0.4

As the surface is rubbed, adsorbate coverages will evolve as a function of the number of passes p. It has been found that methyl thiolates decompose under shear via a first-order reaction:[8-9]

$$\Theta_{th}(p) = \Theta_{th}^{0}\exp(-k_1' p) \qquad \text{(S3)},$$

where $k_1' = k_1 t_C$, where k_1 (with units of s^{-1}) is the first-order rate constant for sliding-induced methyl thiolate decomposition. Since a mechanochemical reaction can only occur when the tip is in contact with a point on the surface, t_C is defined as the time that a point on the surface spends in the contact during each pass and will depend on the contact area and sliding velocity. Both values are kept constant for all experiments carried out in this work, and are identical to those used to measure the rate constants for experiments on the methyl thiolate monolayer.

The mechanochemical decomposition of methyl thiolates results in the formation of gas-phase hydrocarbons and deposits adsorbed sulfur on the surface, which is also removed from the surface by surface-to-bulk transport. Surface-to-bulk transport of sulfur is modeled by a first-order reaction with rate constant k_2.[9-10] The rate equation is therefore:

$$\frac{d\Theta_S}{dt} = k_1\Theta_{th}^{0}\exp(-k_1 t) - k_2\Theta_S \qquad \text{(S4)}.$$

The first term on the right-hand side is due to the addition of sulfur formed by methyl thiolate decomposition, and the second term is due to the removal of adsorbed sulfur by surface-to-bulk transport. This equation is solved to give:

$$\Theta_S(p) = \Theta_S^{0}\exp(-k_2' p) + \frac{\Theta_{th}^{0}k_1'}{(k_2' - k_1')}(\exp(-k_1' p) - \exp(-k_2' p)) \qquad \text{(S5)}$$

where $k_2' = k_2 t_C$. These kinetic equations for an adsorbed overlayer of methyl thiolates are used to model the steady-state kinetics during gas-phase dosing to establish whether these two elementary-step processes, namely mechanochemical methyl thiolate decomposition and surface-to-bulk transport can correctly account for the steady-state reaction.

This is carried out by sequentially applying the equations for each rubbing cycle as outlined below. The initial sulfur coverage for the first pass is zero, but after the first pass ($p = 1$), from Eqn. S5 it becomes:

$$\Theta_S(p = 1) = \frac{\Theta_{th}^0 k_1'}{(k_2' - k_1')}(\exp(-k_1') - \exp(-k_2')) \quad \text{(S6).}$$

From Eqn. S1, the corresponding methyl thiolate coverage after the first pass is given by:

$$\Theta_{th}(p = 1) = \Theta_{th}^0 \exp(-k_1') \quad \text{(S7).}$$

The total concentration of sulfur that has been transported into the subsurface of the copper sample during this first pass ($\chi_{S(sub)}$) is the difference between the initial coverage of methyl thiolate (Θ_{th}^0) and the total coverage of sulfur-containing species after the first pass, $\Theta_{th}(p = 1) + \Theta_S(p = 1)$. As a consequence, the subsurface sulfur concentration after the first pass is given by:

$$\chi_{S(sub)}(p = 1) = \Theta_{th}^0 - \Theta_{th}(p = 1) - \Theta_S(p = 1) \quad \text{(S8).}$$

Sliding during the first pass causes the sulfur to penetrate a distance d_p below the surface. Taking d_0 to be the thickness of the sulfur overlayer gives:

$$\Theta_{S(sub)}(p = 1) = \frac{\chi_{S(sub)}(p=1)}{k_2'} \quad \text{(S9),}$$

where $k_2' = \frac{d_p}{d_0}$.[9] Here, $\Theta_{S(sub)}$ is the proportion of the surface that contains sulfur in the layer below the first layer of copper. This is distinguished from copper sites which have no sulfur atoms in the layer below to take account of the possibility that subsurface sulfur modifies its

friction. Thus, we distinguish four chemical states of the surface; sites covered either by sulfur or methyl thiolate species, which block subsequent methyl thiolate adsorption, and vacant surface sites, some of which have sulfur in the layer below, where DMDS can react to form additional methyl thiolates. The total coverage of sites where methyl thiolate can adsorb is designated Θ_{clean}.

This sets the stage for applying the kinetic model to analyzing the state of the surface during the second pass. Accordingly, the corresponding clean surface coverage after the first pass, $\Theta_{clean}(p=1)$ is given by:

$$\Theta_{clean}(p=1) = 1 - \Theta_{th}(p=1) - \Theta_S(p=1) \qquad \text{(S10)}.$$

The pin then comes out of contact for a period of ~20 seconds, during which additional methyl thiolate adsorbs onto the vacant sites to increase the initial thiolate coverage for the second pass. From Eqns. S1and S10, the uptake of additional methyl thiolate species during the second pass, again assuming Langmuir adsorption kinetics, is given by:

$$\frac{d\Theta_{th}}{dt} = K(1 - \Theta_S(p=1) - \Theta_{th})G \qquad \text{(S11)}.$$

Integrating, as in Eqn. S2, yields:

$$\int_{\Theta_{th}(p=1)}^{\Theta_{th}^0(p=2)} \frac{d\Theta_{th}}{(1-\Theta_S(p=1)-\Theta_{th})} = KG\int_0^{t_{exp}} dt \qquad \text{(S12)},$$

which gives:

$$\Theta_{th}^0(p=2) = \Theta_{th}(p=1) + \Theta_{clean}(p=1)(1-\exp(-KE)) \qquad \text{(S13)}.$$

The term $(1-\exp(-KE))$ is just the coverage that would form on the clean surface after a DMDS exposure of *E* (Langmuir), so that the methyl thiolate coverage increases by an amount $P\Theta_{clean}(p=1)$. *P* is taken to be an adjustable parameter, and from Fig. S3 is expected to lie between ~0.4 and 0.6. Thus, the initial methyl thiolate coverage at the beginning of the second pass $\Theta_{th}^0(p=2) = \Theta_{th}(p=1) + P\Theta_{clean}(p=1)$. This provides the starting methyl thiolate

coverage for calculating coverages during the second pass, where the surface also contains adsorbed and subsurface sulfur from the first pass. From Eqn. S3, the thiolate coverage during the second pass is given by:

$$\Theta_{th}(p=2) = \Theta_{th}^{0}(\mathrm{p}=2)\exp(-k_1') \qquad \text{(S14), and the}$$

sulfur coverage, from Eqn. S5, during the second pass is:

$$\Theta_S(p=2) = \Theta_S(p=1)\exp(-k_2') + \frac{\Theta_{th}^{0}(p=2)k_1'}{(k_2'-k_1')}(\exp(-k_1') - \exp(-k_2')) \qquad \text{(S15).}$$

Again, similarly to Eqn. S8, the subsurface sulfur concentration formed during the second pass is calculated from:

$$\chi_{S(sub)}(p=2) = \Theta_{th}^{0}(p=2) - \Theta_{th}(p=2) - \Theta_S(p=2) \qquad \text{(S16),}$$

and the clean-surface coverage, as in Eqn. S10, gives:

$$\Theta_{clean}(p=2) = 1 - \Theta_{th}(p=2) - \Theta_S(p=2) \qquad \text{(S17).}$$

Now the subsurface coverage includes two contributions; (i) the subsurface sulfur from the first pass that penetrates further into the subsurface region during the second pass, and (ii) subsurface sulfur from the sulfur overlayer that penetrates the subsurface region. It has been shown previously that the distance that the subsurface sulfur penetrates the subsurface region is directly proportional to *p*, so that by analogy to Eqn. S9:

$$\Theta_{S(sub)}(p=2) = \frac{\chi_{S(sub)}(p=2)}{k_2'} + \frac{\chi_{S(sub)}}{2k_2'} \qquad \text{(S18).}$$

These equations can be extended straightforwardly to the n^{th} pass. Based on the equations for p = 2, the initial thiolate coverage before the pin comes into contact for the n^{th} pass becomes:

$$\Theta_{th}^{0}(p=n) = \Theta_{th}(p=n-1) + P\Theta_{clean}(p=n-1) \qquad \text{(S19),}$$

and the corresponding methyl thiolate coverage after sliding during the n^{th} pass is:

$$\Theta_{th}(p=n) = \Theta_{th}^{0}(p=n-1)\exp(-k_1') \qquad \text{(S20),}$$

and the sulfur coverage after the n^{th} pass is:

$$\Theta_S(p=n) = \Theta_S(p=n-1)\exp(-k_2') + \frac{\Theta_{th}^0(p=n-1)k_1'}{(k_2'-k_1')}(\exp(-k_1') - \exp(-k_2')) \quad \text{(S21)}.$$

Again, the subsurface sulfur concentration is:

$$\chi_{S(sub)}(p=n) = \Theta_{th}^0(p=n) - \Theta_{th}(p=n-1) - \Theta_S(p=n-1) \quad \text{(S22)}.$$

Thus, the total concentration of subsurface sulfur that has accumulated after a total of *p* passes is:

$$\chi_{S(sub)}^{tot}(p) = \sum_{n=1}^{p} \chi_{S(sub)}(n) \quad \text{(S22)}.$$

By analogy with Eqn. S18, the subsurface sulfur coverage after a total of *p* passes is given by:

$$\Theta_{S(sub)}(p) = \frac{1}{k_2'}\sum_{m=1}^{p} \frac{\chi_{S(sub)}(p-m)}{(m+1)} \quad \text{(S23)}.$$

Since the rate constant k_1' and k_2' are known,[9] the only unknown fitting parameters are the initial coverage of the methyl thiolate species that form as DMDS dosing is started (Θ_{th}^0) and the value of *P*. Changes in the value of Θ_{th}^0 will predominantly influence the behavior during the first few scans and the subsequent evolution of the surface depends primarily on the value of *P*. However, the uptake curve in Figure S3 allows the values to be constrained to a reasonably narrow range. The kinetic model is tested by calculating the friction coefficient as a function of the number of passes $\mu(p)$ as a function of Θ_{th}^0 and *P* from Eqn. 1 as:

$$\mu(p) = \mu_{th}\Theta_{th}(p) + \mu_S\Theta_S(p) + \mu_{clean}(\Theta_{clean}(p) - \Theta_{S(sub)}) + \mu_{S(sub)}\Theta_{S(sub)}(p) \quad \text{(S24)},$$

which is compared with the experimental results to obtain best-fit values of *P*, Θ_{th}^0 and $\mu_{S(sub)}$.

S3. Subsurface Sulfur Depth Distribution.

In order to calculate the shear-induced sulfur depth profile, the same kinetic model as above is used, which assumes that the film penetrates a distance d_p into the bulk for each pass of the tribopin over the surface. It is assumed that there has been a total of *p* passes over the surface. Since the adsorbed coverages evolve rapidly to a steady-state value (Figure 5), the surface sulfur

coverage is taken to have constant value of Θ_S. The model is illustrated in Figure S4 which shows that a sulfur-covered surface that has been rubbed p times will penetrate a distance pd_p into the sample. Since the amount of sulfur deposited during each cycle is constant, as it spreads through the sample, its concentration (measured in units of sulfur monolayers) decreases. As illustrated in Figure S4, a layer that was rubbed after the sulfur was adsorbed onto the surface during the first pass will have moved a distance pd_p and the concentration will be $\Theta_S/\left(d_p/d_0\, p\right)$ monolayers, where d_0 is the thickness of a sulfur overlayer.

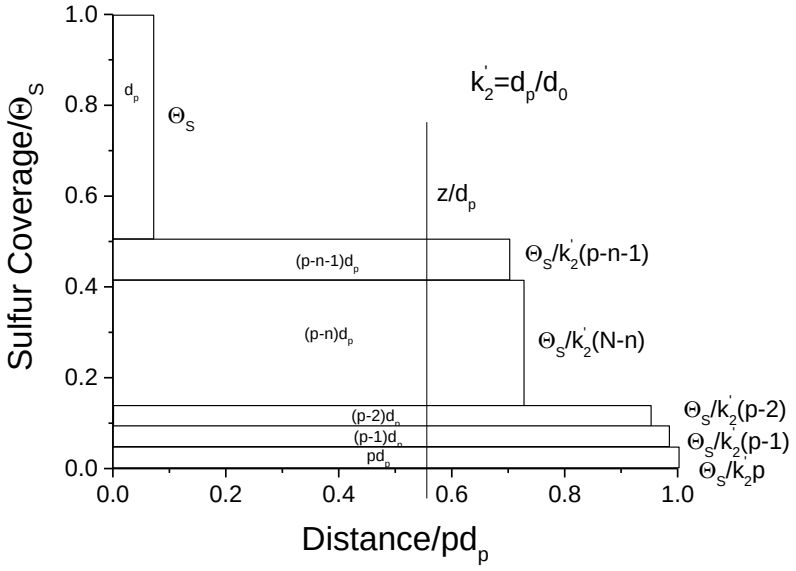

Figure S4. Schematic diagram illustrating the model for surface-to-bulk transport used to calculate the sulfur depth profile.

Correspondingly, a sulfur layer on the surface that is rubbed during the second cycle will have penetrated a distance $(p-1)d_p$ and its concentration will be $\Theta_S/\left(d_p/d_0\,(p-1)\right)$, and a

sulfur overlayer that was rubbed during the n^{th} cycle will have penetrated a distance $(p-n)d_p$ and its concentration will be $\Theta_S / \left({}^{d_p}/_{d_0}\,(p-n) \right)$, and so on.

In order to calculate the sulfur concentration at some depth z below the surface, only those sulfur overlayers that have been rubbed enough times to have penetrated a distance further than z will contribute to the sulfur concentration at this depth, which will have occurred for a number of passes over the surface given by $z = (p-n)d_p$. Thus, all rubbing cycles from $n = 1$ to $n = p - \frac{z}{d_p}$ will contribute to the sulfur coverage, so that the sulfur concentration $C_S(z)$ is given by:

$$C_S(z) = \sum_{n=1}^{p-\frac{z}{d_p}} \frac{\Theta_s}{\left({}^{d_p}/_{d_0}(p-n) \right)} \qquad \text{(S25).}$$

Since Θ_S is taken to be constant, this gives:

$$C_S(z) = \frac{\Theta_s}{\left({}^{d_p}/_{d_0} \right)} \sum_{n=1}^{p-\frac{z}{d_p}} \frac{1}{(p-n)} \qquad \text{(S26).}$$

Putting $\alpha = (p-n)$ gives:

$$C(z) = \frac{\Theta_s}{\left({}^{d_p}/_{d_0} \right)} \sum_{\alpha=p-1}^{\frac{z}{d_p}} \frac{1}{\alpha} \qquad \text{(S27).}$$

As shown previously,[10] this can be summed using the Harmonic number $H_n = \sum_{p=1}^{n} \frac{1}{p}$, so that Eqn. S27 is rewritten as:

$$C_S(z) = \frac{\Theta_s}{\left({}^{d_p}/_{d_0} \right)} \left(\sum_{\alpha=1}^{\frac{z}{d_p}} \frac{1}{\alpha} - \sum_{\alpha=1}^{p-1} \frac{1}{\alpha} \right) \qquad \text{(S28),}$$

and $$C_S(z) = \frac{\Theta_S}{\left(d_p/d_0\right)}\left(H_{\frac{z}{d_p}} - H_p\right) \quad \text{(S29)},$$

where it is assumed that $p \gg 1$. This function has been evaluated in Ref. 10 and gives:

$$C_S(p, z') = \frac{\Theta_S}{(k_s')}\left(ln\left(\frac{p}{z'}\right) - \frac{1}{2}\left(\frac{1}{p} - \frac{1}{z'}\right)\right) \quad \text{(S30)},$$

where $z' = \frac{z}{d_p}$, where $\frac{d_p}{d_0} = k_2'$.

References

1. Furlong, O. J.; Miller, B. P.; Tysoe, W. T., Shear-Induced Surface-to-Bulk Transport at Room Temperature in a Sliding Metal-Metal Interface. *Tribol. Lett.* **2011,** *41*, 257-261.

2. Shirley, D. A., High-Resolution X-Ray Photoemission Spectrum of the Valence Bands of Gold. *Phys. Rev. B* **1972,** *5*, 4709-4714.

3. Briggs, B.; Seah, M. P., *Practical Surface Analysis: Auger and X-ray Photoelectron Spectroscopy*. John Wiley and Sons: New York, **1996**.

4. Scofield, J. H., Hartree-Slater Subshell Photoionization Cross-sections at 1254 and 1487 eV. *J. Electron Spectros. Relat. Phenomena* **1976,** *8*, 129-137.

5. Reilman, R. F.; Msezane, A.; Manson, S. T., Relative Intensities in Photoelectron Spectroscopy of Atoms and Molecules. *J. Electron Spectros. Relat Phenomena* **1976,** *8*, 389-394.

6. Scorciapino, M. A.; Navarra, G.; Elsener, B.; Rossi, A., Nondestructive Surface Depth Profiles from Angle-Resolved X-ray Photoelectron Spectroscopy Data Using the Maximum Entropy Method. I. A New Protocol. *J. Phys. Chem. C* **2009,** *113*, 21328-21337.

7. Seah, M. P.; Dench, W. A., Quantitative Electron Spectroscopy of Surfaces: A Standard Data Base for Electron Inelastic Mean Free Paths in Solids. *Surf. Interface Anal.* **1979,** *1*, 2-11.

8. Adams, H. L.; Garvey, M. T.; Ramasamy, U. S.; Ye, Z.; Martini, A.; Tysoe, W. T., Shear-Induced Mechanochemistry: Pushing Molecules Around. *J. Phys. Chem. C* **2015,** *119*, 7115-7123.

9. Adams, H.; Miller, B. P.; Kotvis, P. V.; Furlong, O. J.; Martini, A.; Tysoe, W. T., In Situ Measurements of Boundary Film Formation Pathways and Kinetics: Dimethyl and Diethyl Disulfide on Copper. *Tribol. Lett.* **2016,** *62*, 1-9.

10. Miller, B.; Furlong, O.; Tysoe, W., The Kinetics of Shear-Induced Boundary Film Formation from Dimethyl Disulfide on Copper. *Tribol. Lett.* **2013,** *49*, 39-46.